Extension to Modified Polar Coordinates and Applications with Passive Measurements

S. N. Balakrishnan*
University of Missouri–Rolla, Rolla, Missouri

A practically successful method to achieve better estimation results for target tracking with passive measurements has been obtained through the use of a set of modified polar coordinates. This state space consists of the reciprocal of the range, the range rate over range, the range acceleration over range, the bearing angle, the bearing-angle rate, and the bearing acceleration, in two dimensions. The elevation angle, its rate, and its acceleration are added to the state space in three dimensions. The performance of this modified polar coordinate filter is superior to that of the widely used rectangular Cartesian coordinate-based extended Kalman filter. Numerical results are obtained by processing the observations made on a single reference trajectory in two dimensions and from a target-intercept problem in three dimensions. Error histories of the range under nominal and off-nominal conditions are presented. Also, the conditions for the observability using passive measurements have been extended to cases where target acceleration is an element of the state space.

I. Introduction

THE problem of estimating the states of a maneuvering target from passive measurements has generated a lot of interest in recent years because of its applications in submarine-tracking and homing-missile guidance.[1–6] A difficulty in obtaining good estimates for the target motion analysis arises from having to use only angular observations (in the case of passive measurements) to extract information about the positions and velocities and, in this study, the target accelerations also. Mathematically, this problem can be described in an inertial rectangular coordinate frame by a linear dynamical model and a discrete nonlinear observation model or in an inertial polar coordinate frame by a nonlinear dynamical model and a linear discrete observation model.

The most widely used method in the applications of nonlinear filtering methods to the tracking problems has been the extended Kalman filter (EKF).[1–5] An approach to achieving a better nonlinear estimator is to select a state space in which improved estimation occurs.[6–10,13] The observability of the passive-tracking problem has also generated some interest. Lindgren and Gong[11] have examined the observability of the bearings-only problem wherein the observer motion is confined to constant velocity segments. Under such conditions, he has shown that the state covariance varies inversely proportional to the number of observer maneuvers. Nardone and Aidala[12] discussed the observability requirements of the bearings-only problem by solving a third-order nonlinear differential equation. Nardone has also proved that for certain types of maneuvers, the estimation process is unobservable, even when the associated bearing rate is nonzero. Aidala and Hammel[7] formulated the target-tracking problem in modified polar coordinate (MPF) to investigate the observability of the state space with bearings-only measurements. Aidala has used a batch filter to show that the target range is unobservable until the observer executes a maneuver. In all of these studies, the states are the positions and the velocities. An important feature of this study is that the state space here includes the positions, velocities, and the target accelerations.

The mathematical formulations of the passive-tracking problem is presented in Sec. II. The conditions for the observability of this extended state space are examined in Sec. III. Two more states are added to the modified polar system used in Ref. 7 to account for the target acceleration in two dimensions, and a modified batch filter[13] is used since the mathematical model is different from that of Ref. 7. The method of derivation of the conditions for the observability of the range follows that of Ref. 7. The numerical experiments and the relevant discussions are presented in Sec. IV, and the conclusions are given in Sec. V.

II. Problem Formulation

Rectangular Coordinates

The target and the observer are represented as point masses in the tracking simulation. The target is assumed to move with a constant velocity. However, in the filtering process, its acceleration has been modeled as a stochastic process to reflect the observer's lack of knowledge about the target motion. The system model is given by

$$\dot{x}(t) = Fx(t) + b(t) + w(t) \tag{1}$$

where $x = [x_R, y_R, \dot{x}_R, \dot{y}_R, a_{T_x}, a_{T_y}]^T$, with the first two variables representing the relative positions, the third and fourth representing the relative velocities, and the last two denoting the target accelerations along x and y axes, respectively.

$$F = \begin{bmatrix} 0 & I & 0 \\ 0 & 0 & I \\ 0 & 0 & \lambda_T \end{bmatrix} \tag{2}$$

with each partition representing a 2×2 matrix. The quantity λ_T is given by

$$\lambda_T = \begin{bmatrix} \lambda_1 & 0 \\ 0 & \lambda_1 \end{bmatrix} \tag{3}$$

Note that when λ_1 is zero, the target motion is a Brownian motion process. The six-element vector b is given by

$$b = [0, 0, a_{M_x}, a_{M_y}, 0, 0]^T \tag{4}$$

where a_{M_x} and a_{M_y} are the components of the observer acceleration in the x and y directions, respectively. The six-element noise vector w has only two nonzero components w_{T_x}

Presented as Paper 87-1025 at the AIAA Aerospace Sciences Meeting, Reno, NV, Jan. 12–15, 1987; received Dec. 10, 1987; revision received July 15, 1988.

*Assistant Professor, Aerospace Engineering. Senior Member AIAA.

and w_{T_y} in the target acceleration dynamics in the x and y directions, respectively.

The measurement model is given by

$$Z_{1i} = \tan^{-1}(y_{R_i}/x_{R_i}) + V_{1i} \tag{5}$$

where Z_{1i} is the discrete measurement at stage i and x_{R_i} and y_{R_i} are the corresponding relative positions. The noise V_{1i} is a white, random sequence, with mean zero and variance V.

Because of the linearity of Eq. (1), the mean states can be propagated in a closed form as

$$x(t) = \phi(t,t_0)x_0 + \int_{t_0}^{t} \phi(t,\tau)b(\tau)\,d\tau \tag{6}$$

where

$$\phi(t,\tau) = \begin{bmatrix} 1 & 0 & (t-\tau) & 0 & \Delta_1\tau & 0 \\ 0 & 1 & 0 & (t-\tau) & 0 & \Delta_1\tau \\ 0 & 0 & 1 & 0 & \Delta_2\tau & 0 \\ 0 & 0 & 0 & 1 & 0 & \Delta_2\tau \\ 0 & 0 & 0 & 0 & \Delta_3\tau & 0 \\ 0 & 0 & 0 & 0 & 0 & \Delta_3\tau \end{bmatrix} \tag{7}$$

$$\Delta_1\tau = \frac{1}{\lambda_1^2}(\exp[-\lambda_1(t-\tau)] + \lambda_1(t-\tau) - 1)$$

$$\Delta_2\tau = -\frac{1}{\lambda_1}[\exp(-\lambda_1(t-\tau)) - 1]$$

$$\Delta_3\tau = \exp[-\lambda_1(t-\tau)]$$

Modified Polar Coordinates

The dynamics of the tracking problem is given by Eq. (1), and the measurement function is described by Eq. (5) in the Cartesian coordinates. However, in order to facilitate the analysis of observability and obtain better performance, the problem is formulated in a modified polar coordinate system which is observed through the following transformation as

$$y = f(x) \tag{8}$$

where

$$y = [y_1,y_2,y_3,y_4,y_5,y_6]^T = \left[\frac{1}{R}, \theta, \frac{\dot{R}}{R}, \dot{\theta}, \frac{\ddot{R}}{R}, \ddot{\theta}\right]^T \tag{9}$$

The expressions for the modified polar coordinates in terms of the Cartesian coordinates are given as

$$R = (x_R^2 + y_R^2)^{1/2} \tag{10a}$$

$$\theta = \tan^{-1}(y_R/x_R) \tag{10b}$$

$$\dot{R} = (x_R\dot{x}_R + y_R\dot{y}_R)/R \tag{10c}$$

$$\dot{\theta} = (x_R\dot{y}_R - \dot{x}_Ry_R)/R^2 \tag{10d}$$

$$\ddot{R} = \frac{\dot{x}_R^2 + \dot{y}_R^2 + x_R\ddot{x}_R + y_R\ddot{y}_R}{R} - \frac{(x_R\dot{x}_R + y_R\dot{y}_R)^2}{R^3} \tag{10e}$$

$$\ddot{\theta} = \frac{R^2(x_R\ddot{y}_R - \ddot{x}_Ry_R) - 2(x_R\dot{y}_R - \dot{x}_Ry_R)(x_R\dot{x}_R + y_R\dot{y}_R)}{R^4} \tag{10f}$$

where

$$\ddot{x}_R = a_{T_x} - a_{M_x} \tag{11}$$

and

$$\ddot{y}_R = a_{T_y} - a_{M_y} \tag{12}$$

The inverse transformation from the set of modified polar coordinates to the Cartesian system is given by

$$x = g(y) \tag{13}$$

where

$$x = [x_R,y_R,\dot{x}_R,\dot{y}_R,a_{T_x},a_{T_y}]^T \tag{14}$$

and

$$g(y) = \begin{bmatrix} (\cos y_2)/y_1 \\ (\sin y_2)/y_1 \\ (y_3\cos y_2 - y_4\sin y_2)/y_1 \\ (y_3\sin y_2 + y_4\cos y_2)/y_1 \\ \frac{1}{y_1}[(y_5 - y_4^2)\cos y_2 - (y_6 + 2y_3y_4)\sin y_2] + a_{M_x} \\ \frac{1}{y_1}[(y_5 - y_4^2)\sin y_2 + (y_6 + 2y_3y_4)\cos y_2] + a_{M_y} \end{bmatrix} \tag{15}$$

III. Analysis of the Observability of the Range

Although the estimators MPF and EKF are useful as recursive sequential online filters, they are not as easily amenable to the analysis of the observability characteristics of the tracking problem as is the batch algorithm, which used all the measurements available at any time to estimate the states at a chosen time instant. The significance of this feature is that the corrections to the state at a chosen time, resulting from information from all the measurements, can be analyzed because all of them are related to that chosen time instant. The method to investigate the observability of the state space of the two-dimensional target-tracking problem is based on Ref. 7 where a similar problem is discussed without modeling the target acceleration as a state. The coordinate system used in this study is an extension of the modified polar coordinates. Two more states are added to the state space to account for the target acceleration. The measurement function is linear in this system and the particular way in which the components of the system have been selected makes the analysis of the observability of the range direct. It is shown that the estimation of the reciprocal of the range (which is a state in the modified polar coordinates) is unobservable under certain conditions.

Analysis of the Observability Using the Batch Process

The batch-estimation algorithm for a general nonlinear problem including the state noise is formulated in Ref. 13. By the examination of the quantities required to update the states in the batch filter, the conditions for the observability of the range can be developed. The update equation for the deviation of the initial state after processing i measurements is given by

$$\hat{y}_0 = \hat{P}_{0i}(H^T\Gamma^{-1}z + \bar{P}_{00}^{-1}\bar{y}_0)$$

where

$P_{0i} \equiv$ the initial state covariance after processing i measurements

$$= [H^T\Gamma^{-1}H + \bar{P}_{00}^{-1}]^{-1} \tag{16}$$

$P_{00} \equiv$ the initial state covariance before processing any measurement

$H \equiv$ the matrix containing all the measurement partial derivatives up to the stage i

$\Gamma \equiv$ the matrix containing the covariances of all the equivalent measurements, z_j, $j = 1,2,\ldots,i$

$$z = [z_1,z_2,\ldots,z_j]^T \tag{17}$$

where z_i is the difference between the observation z_i and the projected measurement θ_i at time i

$$y_0 \equiv \text{the assumed state deviations at stage 0}$$

The uncertainty in the estimate is affected by the information contained in the matrix $H\Gamma^{-1}H$, and, therefore, its content will be examined first. The elements of H are given by

$$H = \begin{bmatrix} H_1 \\ H_2 \\ \cdot \\ \cdot \\ \cdot \\ H_i \end{bmatrix} = \begin{bmatrix} H_1\phi(1,0) \\ H_2\phi(2,0) \\ \cdot \\ \cdot \\ \cdot \\ H_i\phi(i,0) \end{bmatrix} \tag{18}$$

Since the elements of the measurement partial derivative matrix H_j are constant, the matrix product $H_j\phi(j,0)$ is

$$H_j\phi(j,0) = [\phi_{21}(j,0),\phi_{22}(j,0),\phi_{23}(j,0), \phi_{24}(j,0),\phi_{25}(j,0),\phi_{26}(j,0)] \tag{19a}$$

$$H_j(\phi)(j,0) = \left[\frac{\partial y_{2j}}{\partial y_{10}}, \frac{\partial y_{2j}}{\partial y_{20}}, \frac{\partial y_{2j}}{\partial y_{30}}, \frac{\partial y_{2j}}{\partial y_{40}}, \frac{\partial y_{2j}}{\partial y_{50}}, \frac{\partial y_{2j}}{\partial y_{60}}\right] \tag{19b}$$

In order to compute the expressions for the partial derivatives in Eq. (19b), the equation for the bearing angle at any time t is obtained as

$$y_2(t) = \tan^{-1}[y_R(t)/x_R(t)] \tag{20}$$

After some manipulations, Eq. (20) can be written as

$$y_2(t) = y_{20} + \tan^{-1}\left(\frac{NR}{DR}\right) \tag{21}$$

where

$$NR = y_{40}\,\Delta t + \Delta_1\tau(2y_{30}y_{40} + y_{60}) - y_{10}[\Delta_1\tau(a_{M_{x_0}}\sin y_{20} - a_{M_{y_0}}\cos y_{20}) - b_{yy}] \tag{22}$$

$$DR = 1 + y_{30}\,\Delta t + \Delta_1\tau(y_{50} - y_{40}^2) + y_{10}[\Delta_1\tau(a_{M_{x_0}}\cos y_{20} + a_{M_{y_0}}\sin y_{20}) - b_{xx}] \tag{23}$$

and b_{xx} and b_{yy} are defined as

$$b_{xx} \equiv \int_{t_0}^{t}\int_{t_0}^{t} a_{M_x}(\tau)\,d\tau\,dt\cos y_{20} + \int_{t_0}^{t}\int_{t_0}^{t} a_{M_y}(\tau)\,d\tau\,dt\sin y_{20} \tag{24a}$$

$$b_{yy} \equiv \int_{t_0}^{t}\int_{t_0}^{t} a_{M_x}(\tau)\,d\tau\,dt\sin y_{20} - \int_{t_0}^{t}\int_{t_0}^{t} a_{M_y}(\tau)\,d\tau\,dt\cos y_{20} \tag{24b}$$

Note that the partial derivatives of y_{2j} with respect to y_{20} through y_{60} will have nonzero terms even when the observer acceleration components $a_{M_x}(t)$ and $a_{M_y}(t)$ are zero. However, this is not the case with respect to y_{10}. The coefficients of y_{10} in NR and DR contain the observer acceleration terms and they vanish if

$$b_{xx} = \Delta_1\tau(a_{M_{x_0}}\cos y_{20} + a_{M_{y_0}}\sin y_{20}) \tag{25}$$

$$b_{yy} = \Delta_1\tau(a_{M_{x_0}}\sin y_{20} - a_{M_{y_0}}\cos y_{20}) \tag{26}$$

By referring to Eq. (24), where b_{xx} and b_{yy} are defined, it can be seen that these equations are satisfied if 1) the integral b_{xx} and b_{yy} are zero, which implies that the observer acceleration components $a_{M_x}(t)$ and $a_{M_y}(t)$ are zero at all times; or if 2) the observer acceleration behaves as the target model in the filter, constant or otherwise.

When b_{xx} and b_{yy} satisfy Eqs. (25) and (26), the update equation for the initial state can be decoupled as[7]

$$\hat{y}_{10} = \bar{y}_{10}$$

$$\hat{y}_{b0} = (\bar{p}_{20}^{-1} + h_2^T\Gamma^{-1}h_2)^{-1}(h_2\Gamma^{-1}z + \bar{p}_{20}^{-1}\bar{y}_{b0}) \tag{27}$$

where

$$y_{b0} = (y_{20},y_{30},y_{40},y_{50},y_{60})^T$$

Note that h_2 is the contribution of the measurement partial derivatives to the estimate of y_{60} and that the initial covariance $\bar{p}_{00}$ is assumed diagonal—a common practice. The conclusion from Eq. (27) is that the new measurements have no impact on the estimation of y_{10} (or range). Thus, as compared to the results shown in Ref. 7, which require that the observer acceleration be nonzero for the observability of the range, an additional criterion has been derived for the observability of the extended state space that includes the target acceleration.

IV. Numerical Results

Two-Dimensional Tracking

All numerical results have been obtained by processing the observations made on a single reference trajectory, which is given in Fig. 1. The associated bearing-angle history is given in Fig. 2. The target is modeled in the filter as a Brownian motion process (i.e., $\lambda_1 = 0$).

The target motion is generated with constant velocity. In an inertial Cartesian frame, the initial target positions are 500 ft and 2000 ft with velocities of 150 ft/s and -150 ft/s in the x and y directions, respectively. The accelerating observer starts from the origin of the inertial frame with velocities of 60 ft/s and accelerations of 8.1 ft/s^2 in the x and y directions. Although the x component of the observer acceleration remains constant, its y component switches to 4.05 ft/s^2 after 0.5 s. The engagement lasts for 5 s.

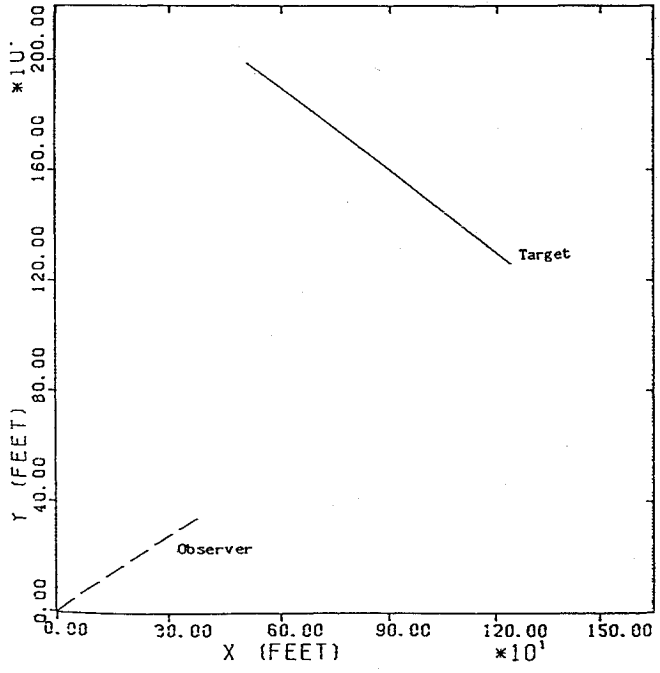

Fig. 1 Engagement history.

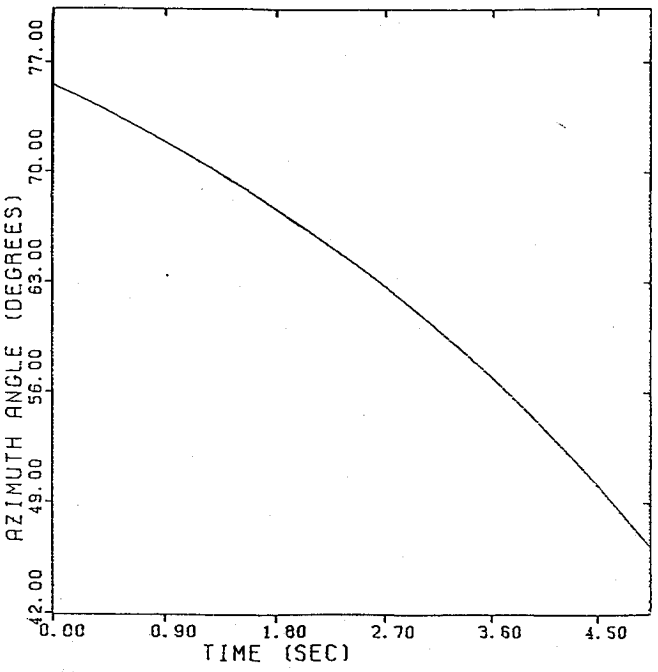

Fig. 2 Measurement angle history.

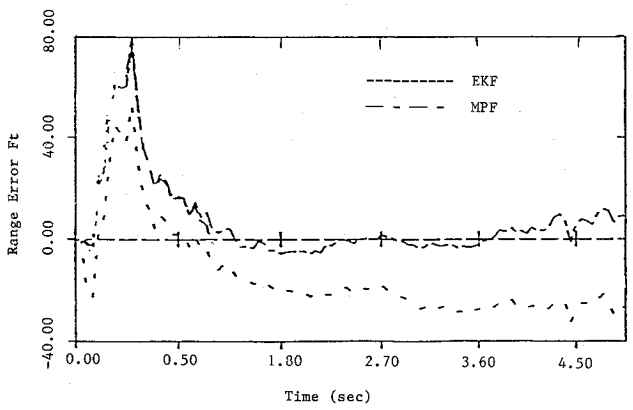

Fig. 3 Range error history (no perturbation).

The initial target state error covariances are 10^4 ft^2 for the positions, 100 ft^2/s^2 for the velocities and 10 ft^2/sec^4 for the accelerations. The acceleration process noise power spectral density is set constant at 10 ft^2/s^5. The measurement frequency is 20 Hz and the measurement error covariance is 10^{-5}. The actual measurements z_i are generated by adding random noise terms to the true measurements. The number of Monte Carlo trials for each case is 20.

Errors in the estimation results are defined as the differences between the magnitudes of the true vectors and the estimated vectors. The range error history for the nominal case is given in Fig. 3. After the initial transients from high gains, the errors in the MPF decrease very fast. Also, the MPF exhibits unbiased error behavior while the EKF seems to be biased.

In practical operating conditions, the filters do not have access to the true conditions and, therefore, cannot be initialized with the true values. In order to assess the merits of the filtering algorithms, then, it is important to analyze their performances under off-nominal conditions.

The results of the simulations with biased initial states are given in Figs. 4 and 5. The error history of the EKF is worse since the linearization assumptions are no longer valid with

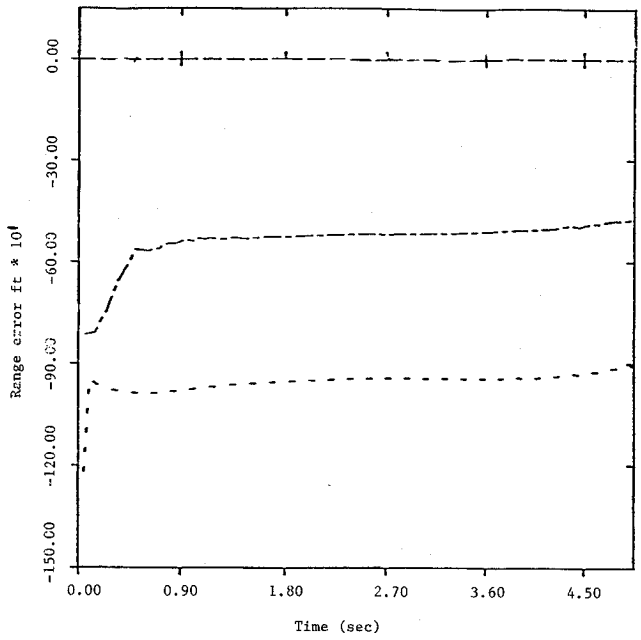

Fig. 4 Range error history ($I = 1500$ ft).

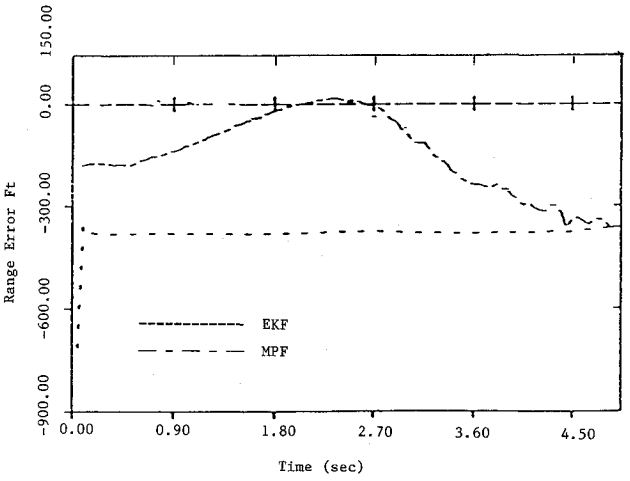

Fig. 5 Range error history ($I = -1500$ ft).

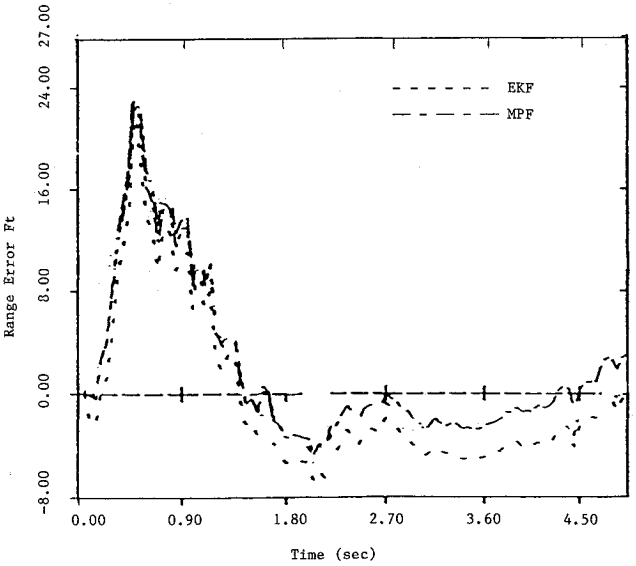

Fig. 6 Range error history ($M = 0.1$).

Table 1 Errors and standard deviation of the EKF ($x_I = x_T + 1000$ ft)

Time, s	$x_T - \hat{x}$	$y_T - \hat{y}$	$\dot{x}_T - \hat{\dot{x}}$	$\dot{y}_T - \hat{\dot{y}}$	$(a_{T_x})_T - \hat{a}_{T_x}$	$(a_{T_y})_T - \hat{a}_{T_y}$
0.00	$-0.2160E+03$	$-0.6327E+03$	$0.4184E-01$	$-0.3164E-01$	$0.1046E-03$	$-0.7909E-04$
0.50	$-0.1499E+03$	$-0.5350E+03$	$-0.1173E+02$	$0.3359E+01$	$-0.4144E+00$	$0.1181E+00$
1.00	$-0.1675E+03$	$-0.5149E+03$	$-0.3070E+02$	$0.1004E+02$	$-0.2052E+01$	$0.6622E+00$
1.50	$-0.1864E+03$	$-0.4998E+03$	$-0.3736E+02$	$0.1348E+02$	$-0.3432E+01$	$0.1228E+01$
2.00	$-0.2068E+03$	$-0.4872E+03$	$-0.4159E+02$	$0.1649E+02$	$-0.4721E+01$	$0.1878E+01$
2.50	$-0.2291E+03$	$-0.4723E+03$	$-0.4643R+02$	$0.2109E+02$	$-0.6481E+01$	$0.3019E+01$
3.00	$-0.2534E+03$	$-0.4617E+03$	$-0.4987E+02$	$0.2242E+02$	$-0.6504E+01$	$0.2942E+01$
3.50	$-0.2790E+03$	$-0.4467E+03$	$-0.5367E+02$	$0.2607E+02$	$-0.7027E+01$	$0.3657E+01$
4.00	$-0.3042E+03$	$-0.4250E+03$	$-0.5678E+02$	$0.3264E+02$	$-0.7448E+01$	$0.5166E+01$
4.50	$-0.3262E+03$	$-0.3939E+03$	$-0.5768E+02$	$0.4229E+02$	$-0.7252E+01$	$0.7307E+01$
5.00	$-0.3451E+03$	$-0.3560E+03$	$-0.5683E+02$	$0.5304E+02$	$-0.6542E+01$	$0.9341E+01$
Time, s	σ_x	σ_y	$\sigma_{\dot{x}}$	$\sigma_{\dot{y}}$	$\sigma_{a_{T_x}}$	$\sigma_{a_{T_y}}$
0.00	$0.1958E+03$	$0.2588E+03$	$0.1026E+02$	$0.1026E+02$	$0.3325E+01$	$0.3325E+01$
0.50	$0.7253E+01$	$0.2294E+02$	$0.9137E+01$	$0.1033E+02$	$0.4035E+01$	$0.4039E+01$
1.00	$0.7736E+01$	$0.2376E+02$	$0.6383E+01$	$0.1057E+02$	$0.4594E+01$	$0.4640E+01$
1.50	$0.9230E+01$	$0.2508E+02$	$0.6038E+01$	$0.1125E+02$	$0.4996E+01$	$0.5151E+01$
2.00	$0.1149E+02$	$0.2744E+02$	$0.7040E+01$	$0.1217E+02$	$0.5173E+01$	$0.5554E+01$
2.50	$0.1458E+02$	$0.3057E+02$	$0.8519E+01$	$0.1308E+02$	$0.5194E+01$	$0.5817E+01$
3.00	$0.1861E+02$	$0.3429E+02$	$0.1033E+02$	$0.1392E+02$	$0.5313E+01$	$0.5964E+01$
3.50	$0.2363E+02$	$0.3830E+02$	$0.1246E+02$	$0.1461E+02$	$0.5620E+01$	$0.6010E+01$
4.00	$0.2943E+02$	$0.4179E+02$	$0.1477E+02$	$0.1477E+02$	$0.6040E+02$	$0.5918E+01$
4.50	$0.3543E+02$	$0.4369E+02$	$0.1690E+02$	$0.1406E+02$	$0.6448E+01$	$0.5692E+01$
5.00	$0.4088E+02$	$0.4320E+02$	$0.1850E+02$	$0.1246E+02$	$0.6745E+02$	$0.5441E+01$

Table 2 Errors and standard deviations of the MPF ($x_I = x_T + 1000$ ft)

Time, s	$x_T - \hat{x}$	$y_T - \hat{y}$	$\dot{x}_T - \hat{\dot{x}}$	$\dot{y}_T - \hat{\dot{y}}$	$(a_{T_x})_T - \hat{a}_{T_x}$	$(a_{T_y})_T - \hat{a}_{T_y}$
0.00	$-0.1134E+03$	$-0.4510E+03$	$-0.1182E+02$	$0.1499E+02$	$-0.2261E+01$	$0.2425E+01$
0.50	$-0.7981E+02$	$-0.2713E+03$	$-0.1937E+02$	$0.1178E+02$	$-0.1666E+01$	$0.1803E+01$
1.00	$-0.9075E+02$	$-0.2697E+03$	$-0.2007E+02$	$0.1280E+02$	$-0.1726E+01$	$0.1804E+01$
1.50	$-0.1037E+03$	$-0.2743E+02$	$-0.2040E+02$	$0.1359E+02$	$-0.1484E+01$	$0.1710E+01$
2.00	$-0.1142E+03$	$-0.2680E+03$	$-0.2099E+02$	$0.1417E+02$	$-0.1320E+01$	$0.1620E+01$
2.50	$-0.1252E+03$	$-0.2574E+03$	$-0.2284E+02$	$0.1685E+02$	$-0.2225E+01$	$0.2206E+01$
3.00	$-0.1367E+03$	$-0.2496E+03$	$-0.2364E+02$	$0.1689E+02$	$-0.1895E+01$	$0.1840E+01$
3.50	$-0.1489E+03$	$-0.2392E+03$	$-0.2498E+02$	$0.1928E+02$	$-0.2221E+01$	$0.2319E+01$
4.00	$-0.1597E+03$	$-0.2233E+03$	$-0.2578E+02$	$0.2342E+02$	$-0.2473E+01$	$0.3308E+01$
4.50	$-0.1673E+03$	$-0.2018E+03$	$-0.2527E+02$	$0.2857E+02$	$-0.2304E+01$	$0.4452E+01$
5.00	$-0.1747E+03$	$-0.1795E+03$	$-0.2454E+02$	$0.3322E+02$	$-0.1987E+01$	$0.5195E+01$
Time, s	σ_x	σ_y	$\sigma_{\dot{x}}$	$\sigma_{\dot{y}}$	$\sigma_{a_{T_x}}$	$\sigma_{a_{T_y}}$
0.00	$0.8000E+02$	$0.3145E+03$	$0.1318E+02$	$0.1334E+02$	$0.3435E+01$	$0.3558E+01$
0.50	$0.4243E+02$	$0.1537E+03$	$0.8030E+01$	$0.1114E+02$	$0.3865E+01$	$0.3834E+01$
1.00	$0.3399E+02$	$0.1054E+03$	$0.7363E+01$	$0.1140E+02$	$0.4492E+01$	$0.4466E+01$
1.50	$0.3570E+02$	$0.9578E+02$	$0.8164E+01$	$0.1233E+02$	$0.4976E+01$	$0.5031E+01$
2.00	$0.3909E+02$	$0.9164E+02$	$0.9372E+01$	$0.1332E+02$	$0.5139E+01$	$0.5443E+01$
2.50	$0.4316E+02$	$0.8880E+02$	$0.1076E+02$	$0.1415E+02$	$0.5123E+01$	$0.5692E+01$
3.00	$0.4786E+02$	$0.8684E+02$	$0.1233E+02$	$0.1488E+02$	$0.5220E+01$	$0.5853E+01$
3.50	$0.5322E+02$	$0.8499E+02$	$0.1426E+02$	$0.1558E+02$	$0.5556E+01$	$0.5899E+01$
4.00	$0.5884E+02$	$0.8225E+02$	$0.1634E+02$	$0.1595E+02$	$0.6003E+01$	$0.5785E+01$
4.50	$0.6391E+02$	$0.7753E+02$	$0.1811E+02$	$0.1581E+02$	$0.6413E+01$	$0.5540E+01$
5.00	$0.6826E+02$	$0.7096E+02$	$0.1938E+02$	$0.1536E+02$	$0.6698E+01$	$0.5333E+01$

large state deviations. A representative sample of the error in the states and the standard deviations of the two filters are compared in Tables 1 and 2.

It can be noted that the covariance generated by the EKF is lower than the MPF. It has been shown in the literature[14-16] that the EKF tends to calculate lower values of the error covariances as compared to the Gaussian second-order filter, truncated second-order filter, and the modified second-order filter. With smaller covariances, the EKF assumes that the estimates are better than they are and gains on the new measurements become smaller. As a result, the incoming observations are underweighted leading to poorer estimates. The error histories of the MPF are better than that of the EKF in both cases as can be seen from Figs. 4 and 5.

The range error histories of the filters with mismatched measurement covariances are given in Figs. 6 and 7. The measurement covariance mismatch is defined as the ratio of the actual measurement covariance to the filter computed value. Both the MPF and the EKF show similar responses to a mismatch of 0.1 (less noisy observations). The error histories corresponding to a higher mismatch of 10 (very noisy) show the superiority of the MPF. The MPF does not show any deterioration caused by the noisy data, while the performance of EKF shows degradation with time.

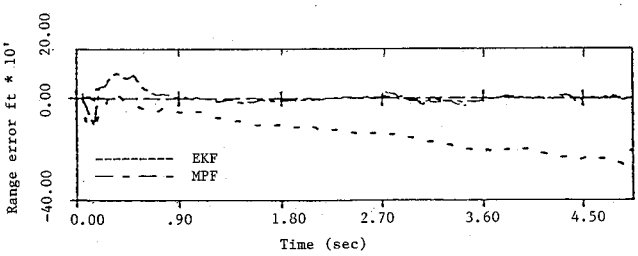

Fig. 7 Range error history ($M = 10$).

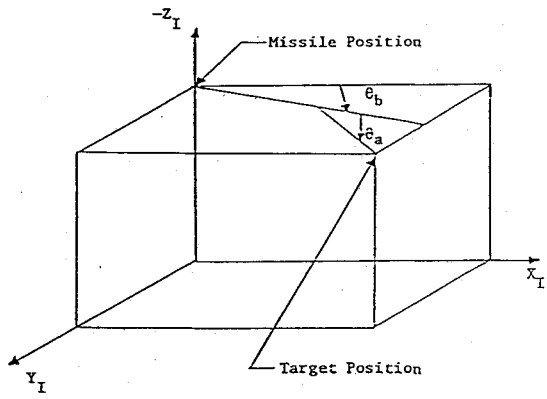

Fig. 8 Launch geometry.

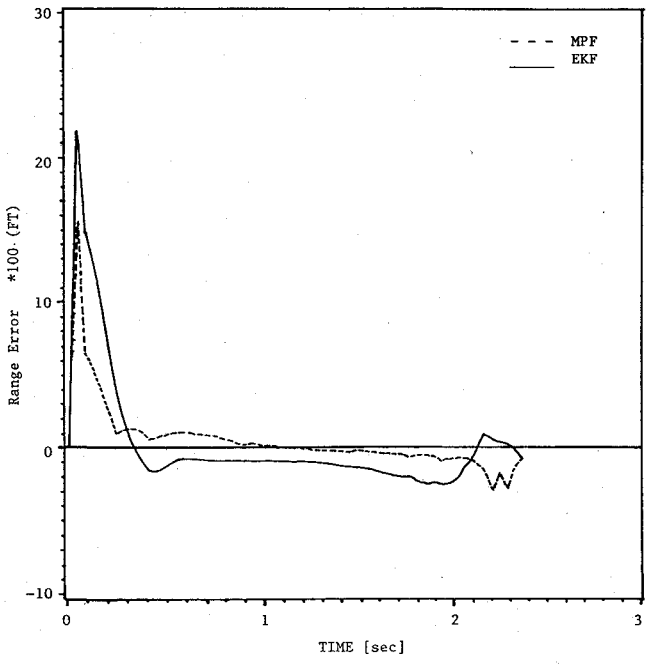

Fig. 9 Range error history (no perturbation).

Three-Dimensional Target-Intercept Problem

The second application of interest is a target-intercept problem.[3] The state space consists of the relative position, relative velocity, and the target acceleration in all the three dimensions bringing the dimension of the state space to nine. The target motion is modeled in the filter as a first-order Markov process. The additional measurement is the elevation angle given by

$$Z_{2_i} = \tan^{-1}\left(\frac{-Z_{Ri}}{\sqrt{x_{R_i}^2 + y_{R_i}^2}}\right) + v_{2i}$$

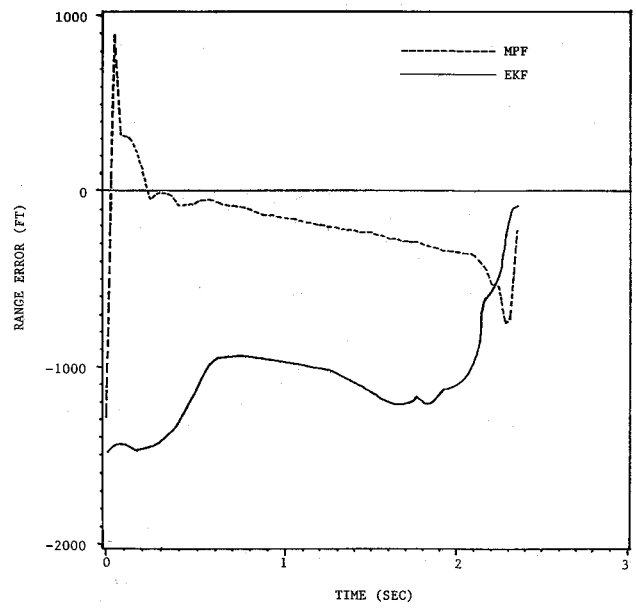

Fig. 10 Range error history ($I = 1000$ ft).

where Z_{R_i} is the relative position in the Z direction and v_{2i} is a zero-mean white noise sequence. The guidance scheme to compute the commanded missile acceleration has been based on an "optimal" linear guidance law.[1,3,6]

The launch geometry used in this analysis is described in Fig. 8. For this inertial system, the Z_1 axis is directed toward the Earth's center, the X_1 axis is aligned parallel with the missile's initial launch direction, and the Y_1 axis is chosen to make the inertial system right handed. The engagement geometry used in this analysis is characterized by the initial conditions: range 3000 ft; altitude 10,000 ft; aspect angle θ_a 60 deg; and offboresight angle θ_b 0.0 deg. The initial state covariances are set to 10^7 ft^2 for the relative positions, 100 ft^2/s^2 for the relative velocities, and 10 ft^2/s ft for the target accelerations, respectively. The power spectral density of the target acceleration process noise is set at 50,000 ft^2/s^5.

The range error history for the nominal case is given in Fig. 9; the case where the filter initial conditions offset by 1000 ft is given in Fig. 10. As in the two-dimensional example, the MPF shows a more *unbiased* and a better tracking performance as compared to the EKF.

V. Conclusions

The problem of estimating the states of a manuevering target from passive measurements has been considered. A set of modified polar coordinates has been used for estimation. Two conditions for the observability of the target-tracking problem, where the target acceleration is contained in the state space and the bearings are the only measurements, have been derived. The performance of the modified polar coordinate has been shown to be superior to that of the rectangular Cartesian coordinate-based extended Kalman filter under nominal as well as off-nominal conditions.

References

[1]Fiske, P. H., "Advanced Digital Guidance and Control Concepts for Air-to-Air Tactical Missiles." U.S. Air Force Armanent Lab., Armanent Development and Test Center, Eglin AFB, FL, Rept. AFATL-TR-77-130, Dec. 1977.

[2]Singer, R., "Estimating Optimal Tracking Filter Performance for Manned Maneuvering Targets," *IEEE Transactions on Aerospace Electronics Systems*, Vol. AES-6, July 1970, pp. 473–483.

[3]Sammons, J. M., Balakrishnan, S., Speyer, J. L., and Hull, D. G., "Development and Comparison of Optimal Filters," Air Force Armament Lab., U.S. Air Force Systems Command, Eglin AFB, FL, Rept. AFATL-TR-79-87, Oct. 1979.

[4]Titus, H. (ed.), *Advances in Passive Target Tracking*, Vol. I, Naval Post Graduate School, Monterey, CA, NPS-62TS77071, May 1977.

[5]Tapley, B. D., Abusali, P. A. M., and Schutz, B. E., "Estimating the Motion of Maneuvering Targets Using Passive Measurements," Institute of Advanced Study in Orbital Mechanics, Univ. of Texas, Austin, TX, IASOM-TR-SO-2, Aug. 1980.

[6]Balakrishnan, S. N. and Speyer, J. L., "A Coordinate Transformation-Based Filter for Improved Target Tracking," *Journal of Guidance, Control, and Dynamics*, Vol. 9, Nov.–Dec. 1986, pp. 704–709.

[7]Aidala, V. J. and Hammel, S. E., "Utilization of Modified Polar Coordinates for Bearings-Only Tracking," *IEEE Transactions on Automatic Control*, Vol. AC-28, March 1983, pp. 283–293.

[8]Tenney, R. R., Herbert, R. S., and Sandell, N. R., "A Tracking Filter for Maneuvering Sources," *IEEE Transactions on Automatic Control*, Vol. AC-22, April 1977, pp. 246–251.

[9]Weiss, H. and Moore, J. B., "Improved Extended Kalman Filter Design for Passive Tracking," *IEEE Transactions on Automatic Control*, Vol. AC-25, Aug. 1980, pp. 807–811.

[10]Mehra, R. K., "A Comparison of Several Nonlinear Filters for Re-entry Vehicle Tracking," *IEEE Transactions on Automatic Control*, Vol. AC-6, Aug. 1971, pp. 307–319.

[11]Lindgren, A. G. and Gong, K. F., "Properties of a Bearings-Only Motion Analysis Estimator: An Interesting Case Study in System Observability," *Proceedings of 12th Asilomar Conference on Circuits, Systems, and Computers*, Western Periodicals, North Hollywood, CA, Nov. 1978, pp. 50–58.

[12]Nardone, S. C. and Aidala, V. I., "Observability Criteria for Bearings-Only Target Motion Analysis," *IEEE Transactions on Aerospace and Electronic Systems*, Vol. AES-17, March 1981, pp. 162–165.

[13]Balakrishnan, S. N., "Development of Two Maximum-Likelihood Filters and Their Applications to Tracking Problems," Ph.D. Dissertation, Dept. of Aerospace Engineering and Engineering Mechanics, Univ. of Texas, Austin, TX, May 1984.

[14]Jazwinski, A., *Stochastic Processes and Filtering Theory*, Academic, New York, 1970.

[15]Sorenson, H. W. and Stubberud, H. W., "Nonlinear Filtering by Approximation of the Posteriori Density," *International Journal of Control*, Vol. 8, July 1968, pp. 33–51.

[16]Denham, D. F. and Pines, S., "Sequential Estimation When Measurement Function Nonlinearity Is Comparable to Measurement Error," *AIAA Journal*, Vol. 4, June 1966, pp. 1071–1076.